Physica Medica xxx (2016) xxx–xxx

Contents lists available at ScienceDirect

Physica Medica

journal homepage: http://www.physicamedica.com

Original paper

Dosimetric and bremsstrahlung performance of a single convergent beam for teletherapy device

R.G. Figueroa [a,b,*], M. Santibáñez [a,b], M. Valente [c,a,b]

[a] Departamento de Ciencias Físicas, Universidad de La Frontera, Temuco, Chile
[b] Centro de Física e Ingeniería en Medicina – CFIM, Universidad de La Frontera, Temuco, Chile
[c] Instituto de Física E. Gaviola, CONICET & Universidad Nacional de Córdoba, Argentina

ARTICLE INFO

Article history:
Received 20 May 2016
Received in Revised form 1 October 2016
Accepted 4 October 2016
Available online xxxx

Keywords:
Convergent beam radiotherapy (CBRT)
Monte Carlo simulations
Dosimetry

ABSTRACT

The present work investigates preliminary feasibility and characteristics of a new type of radiation therapy modality based on a single convergent beam of photons. The proposal consists of the design of a device capable of generating convergent X-ray beams useful for radiotherapy. The main goal is to achieve high concentrated dose delivery. The first step is an analytical approach in order to characterize the dosimetric performance of the hypothetical convergent photon beam. Then, the validated FLUKA Monte Carlo main code is used to perform complete radiation transport to account also for scattering effects. The proposed method for producing convergent X-rays is mainly based on the bremsstrahlung effect. Hence the operating principle of the proposed device is described in terms of bremsstrahlung production. The work is mainly devoted characterizing the effect on the bremsstrahlung yield due to accessories present in the device, like anode material and geometry, filtration and collimation systems among others.

The results obtained for in-depth dose distributions, by means of analytical and stochastic approaches, confirm the presence of a high dose concentration around the irradiated target, as expected. Moreover, it is shown how this spot of high dose concentration depends upon the relevant physical properties of the produced convergent photon beam.

In summary, the proposed design for producing single convergent X-rays attained satisfactory performance for achieving high dose concentration around small targets depending on beam spot size that may be used for some applications in radiotherapy, like radiosurgery.

1. Introduction

Teletherapy modalities have been typically implemented in clinics by linear accelerators or cobalt units for some time. Both these techniques use photon beams, which are produced with an inherent divergent nature. Then, high dose concentrations are usually achieved by superposition of several incident fields in order to minimize radiation to healthy tissues and organs. Modern methodologies like intensity modulated radiotherapy (IMRT) [1,2] attempt to deliver higher radiation dose levels with improved capability for tumor targeting while doses delivered to surrounding critical structures are kept as low as possible [2,3].

Recent technological developments like Cyber-knife [4], TrueBeam [5] or tomotherapy [6] are capable of attaining high-dose gradients to achieve dose escalation within the irradiation volume. The complexity of these kinds of technologies and specially their cost might constitute a drawback for large-scale worldwide implementation. Hence, it appears suitable to consider a photon beam of inherent convergent characteristics that could attain similar or even better dosimetric performance for treatment requiring high dose concentration [7,8]. The main characteristics of such a technology have been already well described and specific details are available in literature [9]. The present work is focused on the most relevant features of the bremsstrahlung yield corresponding to the specific setup of this new strategy for radiation delivery by means of convergent X-ray beams. The main characteristics of the proposed device, some of the accessories and a preliminary prototype for the device are described in detail in the corresponding patent and previous works [9,10]. In this context, the present work refers to the characteristics of the bremsstrahlung yield that constitutes the convergent beam.

* Corresponding author at: Departamento de Ciencias Físicas, Universidad de La Frontera, Temuco, Chile.
E-mail address: rodolfo.figueroa@ufrontera.cl (R.G. Figueroa).

http://dx.doi.org/10.1016/j.ejmp.2016.10.003
1120-1797/

2. Materials and methods

The proposal for generating convergent X-ray beams is mainly based on a suitable manipulation of the electron beam produced by clinical linear accelerators that typically operate with energies larger than 6 MeV. The starting point consists of achieving perpendicular incidence of the electron beam in a relatively thin (⩽3 mm) spherical tungsten shell (20 cm in diameter, approximately) that constitutes the target. As a consequence of the impact of electrons, bremsstrahlung radiation is generated and is directed mainly forward. Then, the desired convergent effect should be observed [9,10]. This effect is produced, because of the properties of bremsstrahlung angular distribution causing the majority of radiation emissions to travel directly to the focal spot located at the centre of the spherical shell. This issue must be checked for different energies of the electron beam, and, naturally, for different prototype designs. However, it might be expected that the effect is less likely for the lowest energies, due to inherent properties of bremsstrahlung production.

Once bremsstrahlung is generated, the convergence of the photon beam must still be improved. Some accessories, like collimation and filter systems, are included in the prototype for this purpose.

The whole procedure can be summarized as follows: the electron beam is produced by the standard linear accelerator, thus making it possible to achieve energies in the megavoltage range. The electron beam interacts with a bending/splitting system consisting of an electron-dispersive sheet and/or electromagnetic deflector that guides the electron beam with the aim of attaining a normal impact on the target (shell anode) by means of electrostatic and/or magnetic devices. Photons emerge from the anode shell pointing in the same direction of incident electrons. They then pass through a filter and, finally, a curved multiple-collimation system acts as an ulterior accessory for improving beam convergence.

Moreover, it is clear that such a device has the capability of generating single convergent beams using the entire target for electron impact or limiting the process to a specific region. The effect of limiting the region of impact may affect mainly the dosimetric performance outputs, like entrance-to-peak dose ratio.

The emerging photon beam is emitted mainly convergently, despite the location where electrons reach the shell anode. Finally, the focus of the emerging convergent photon beam is geometrically determined by shell pieces, namely the anode, collimation grid and filtration accessories. Further details are available in previous works [9,10].

Of course, it is not possible to ensure that all photon fluence will arrive at the phantom, because of the losses in filtration and collimation systems. Therefore, it becomes crucial to characterize the bremsstrahlung yield according to the actual design of the proposed prototype. As is well-known, the angular distribution and kinetic energy of bremsstrahlung production are intrinsically coupled so that it is necessary to investigate both of these parameters simultaneously affecting bremsstrahlung yield. The key is that angular distribution probabilities become more and more closely concentrated around forward direction for higher electron kinetic energies in the megavoltage range.

Bremsstrahlung yield produced by high energy electrons striking high atomic number (Z) targets has been thoroughly investigated and is explained in detail in the basic literature [11,12] and the formulation describing the process for this convergent photon beam prototype was already presented showing that the bremsstrahlung yield, described in terms of the double differential cross section $\left(\frac{d^2\sigma_{Br}}{dEd(\cos\theta)}\right)$ is determined by [9,13]:

$$\frac{d^2\sigma_{Br}}{dEd(\cos\theta)} = \frac{Z^2}{\beta^2} \times \frac{1}{E} A(Z, T, E/T) \left[\frac{\sigma_I(1-(\cos\theta)^2) + \sigma_{II}(1+(\cos\theta)^2)}{\sigma_I(1-\beta(\cos\theta)^2)}\right] \quad (1)$$

In the above equation E is the kinetic energy of the emitted photon produced by electrons with kinetic energy T and velocity v, $A(Z, T, \kappa)$ is a parameter dependent on the target material, $\beta = v/c$ and the coefficients σ_I and σ_{II} (independent of polar angle θ) are obtained from Sommerfeld's model [13,14].

Knowing the characteristics of photon beams generated by bremsstrahlung for both divergent (standard) and convergent arrangements, it remains necessary to investigate the corresponding dosimetric outputs according to the possible options for the prototype. Thus, analytical and Monte Carlo (MC) simulations methods can be adapted for in-phantom dose distribution calculations. As a first approach, isotropic homogeneous water-equivalent medium was selected for the irradiated phantom. If required, dedicated techniques can be developed to calculate dose distribution in anthropomorphic heterogeneous phantoms.

The basic idea for the analytical approach is relatively intuitive and considers that dose concentration can be achieved by combining multiple radiation fields or using beam modulation mechanisms [9,10]. Due to continuity requirements, the absorbed dose due to primary particles calculated at depth ($D(h)$) can be approximated by [9]:

$$D(h) \approx D_0 \frac{L_0^2}{(L_0 - h)^2} e^{-\sum_{ip_i} \mu_i(E_i)\rho h} \quad (2)$$

where L_0 is the focus-surface distance, D_0 is the entrance dose, μ_i is the attenuation coefficient evaluated for the i spectral channel (E_i) of the incident beam (which probability is $p(E_i)$) and ρ is the mass density of the medium. Although expression (2) means that absorbed dose tends to infinity when the depth $h \to L_0$ this hypothetical case does not represent drawbacks or limitation in practice for typical clinical depths.

On the other hand, full radiation transport is performed by means of built-in MC subroutines developed to compute 3D absorbed dose distributions. Hence, mean absorbed dose $\langle D \rangle$ and corresponding uncertainty, typically characterized by standard deviation σ_D are calculated for each voxel according to:

$$\langle D \rangle = \frac{1}{m(i,j,k)} \left[\sum_{prim} E^{(in)}(i,j,k) - \sum_{seco} E^{(out)}(i,j,k)\right] \quad (3)$$

In the above expression (i, j, k) indicated spatial coordinates of the considered voxel of mass $m(i, j, k)$. The quantities $E^{(in)}$ (i, j, k) and $E^{(out)}$ (i, j, k) are the energy deposited in the (i, j, k) voxel due to incoming primary (*prim*) particles and the energy that leaves the voxel due to secondary radiation (*seco*), respectively.

The MC subroutines are based on the FLUKA main code [15,16], which accounts for atomic and also nuclear type interactions. The setups for simulation exactly reproduce geometrical and physical properties of the proposed prototype.

Different kinetic energy values for the electron beam were carefully investigated, paying specific attention to the range of 0.4–10 MeV (0.4, 0.6, 1.0, 1.5, 2.0, 3.0, 4.0, 5.0, 6.0, 8.0 and 10.0 MeV), as might be the interest for the convergent device. MC simulations are divided into two different groups: studies for the effect of accessories on bremsstrahlung yield and those dedicated to dosimetry calculation. After preliminary tests, it was observed that 5×10^8 and 2×10^9 primary showers ensure in all investigated

Please cite this article in press as: Figueroa RG et al. Dosimetric and bremsstrahlung performance of a single convergent beam for teletherapy device. Phys. Med. (2016), http://dx.doi.org/10.1016/j.ejmp.2016.10.003

cases relative standard deviation less than 0.1%, for the first and second group of simulations, respectively.

The MC simulations were carried out for a thin target in the shape of a large, spherical cap. Once performed the first step of MC simulations consisting of the production of the convergent photon beam, the second step was dedicated to the study of the corresponding dosimetric performance. This goal was accomplished irradiating a cubic (200 mm side) water-equivalent phantom centred at focal spot of convergent beam. As output of the first step, the phase state [17] $\Psi(\boldsymbol{r}, E, \boldsymbol{\Omega}, t)$ of emerging particles was obtained, as a function of position $\boldsymbol{r}$, kinetic energy E, direction of movement $\boldsymbol{\Omega}$ and time t. The phase state was calculated for particles leaving the shielding head (Fig. 1).

All the interaction mechanisms of the bremsstrahlung radiation with the phantom are taken into consideration for different configurations considered for MC simulations, like kinetic energy of incident electrons, geometrical and physical characteristics of target-filter-collimation device, as sketched in Fig. 1.

Specially adapted subroutines have been developed based on the FLUKA main code. Simulation setup arrangements reproduce exactly both the geometrical and physical radiation transport properties considered for the analytical model, in order to consider converging bremsstrahlung photons arising from a suitable emission shell and respective collimation devices.

The implemented simulation mechanism allows the calculation of dosimetric performance as well as other physical properties by means of different user-defined configurations for the emission source, such as collimator aperture and anode size. Different

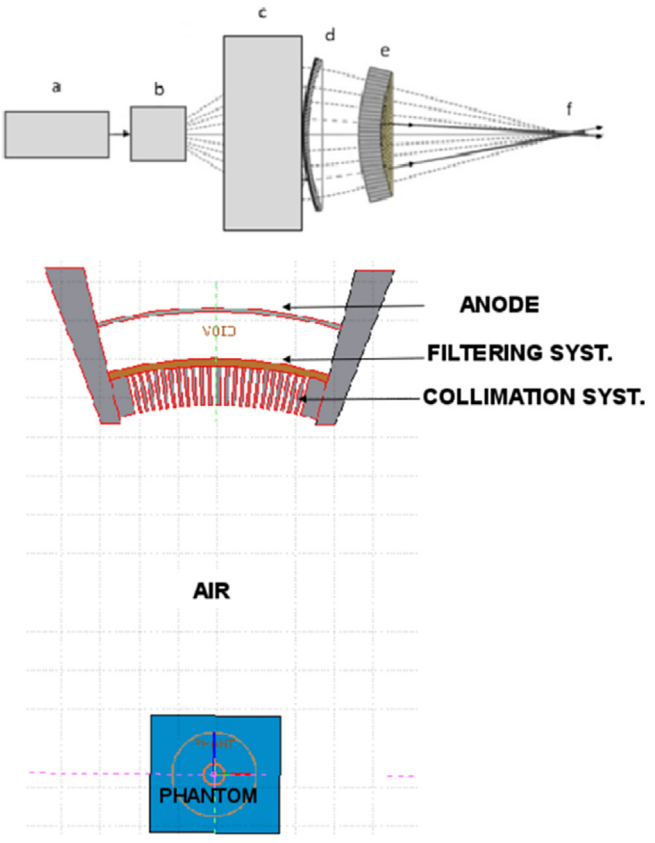

Fig. 1. Sketch of the proposed prototype (top) showing electron source (*a*), devices to manipulate electron beam trajectory (*b*) and (*c*), target (*d*), filtration and collimation systems (*e*) and focal spot (*f*) along with the geometry considered for MC simulations (bottom) showing schematically some of the main components: shielding head containing anode, filtration and collimation systems as well as water-equivalent phantom centred at focal spot for dosimetry purposes.

energy values have been studied for the collision of the incident electron beam with different targets. Additionally, the effect of filtration and collimation systems was investigated. MC simulations have been carried out for 5×10^8 primary showers to ensure good enough uncertainty levels (a standard deviation of less than 0.1% in all cases).

MC simulations started with the incident electron beam that was transported in vacuum before impacting perpendicularly in different positions (uniformly distributed) in the anode target, whereas photons from the bremsstrahlung yield and secondary particles were fully transported in the corresponding materials that include the high Z parts of the X-ray production device, air and water. Both electrons and photons were transported up to 1 keV, which was selected as absorption cut-off energy. The residual energy was considered to be locally deposited.

3. Results

One of the main relevant parts of the prototype is the anode. It is therefore necessary to investigate the effects due to its characteristics, like material and thickness. In fact, as established in expression (1), it is clear that materials with high atomic number represent more convenient options to be investigated. After exhaustive tests, it is found that tungsten exhibits good properties both for bremsstrahlung production as well as favorable properties like high fusion temperature, which is required due to thermal transfer from electron beam.

As an example of the influence of anode thickness, Fig. 2 reports the results for tungsten anode obtained with the FLUKA code. The calculation of the bremsstrahlung yield corresponds to the integration for all emission directions. Similarly, Fig. 2 reports also the angular distribution of bremsstrahlung yield according to angular dependence of double differential cross section $\left(\frac{d^2\sigma_{Br}}{dEd\Omega}\right)$.

Table 1 reports the relative photon flux at focal spot for different apertures of conical septa shown in Fig. 1. This shows that the bremsstrahlung production is high enough even for a very reduced angular aperture collimator cones. Aperture of septa is evaluated in terms of the angle projected at focal spot, which depends upon diameter of circular pin-holes as well as thickness of collimation thickness.

It is crucial for the proposed prototype to produce bremsstrahlung photons mainly in the forward direction. As established in expression (1), angular distribution depends simultaneously on anode material and electron beam energy. Hence, the influence of varying the energy was investigated in detail.

There is a specific relationship between electron energy and tendency to emit photons in a forward manner, which anticipates that higher electron energies increase the concentration of bremsstrahlung yield in the forward direction, as summarized in Fig. 3. Here are also reported the obtained results for the total bremsstrahlung emission as a function of the electron energy. The dose rate output of the prototype is dependent upon electron beam energy, among other design parameters.

Error bars in the total flux (Fig. 3 right) correspond to dispersion (1 standard deviation) due to consideration of a set of 3 different combinations for materials and thicknesses for the filtration system (10–20 mm of Al, Cu or Fe). After detailed characterization of bremsstrahlung production, the study focused on the effects of the inclusion of grid collimation systems. Combinations of different materials (Fe, W and Pb), designs (circular, conical, rectangular) and dimensions (aperture and length) were investigated to establish the best performance.

The design of the prototype takes into account, as a priority, the physical properties of the radiation output at the isocenter where dosimetric performance needs to be accurately controlled. Fig. 4

Please cite this article in press as: Figueroa RG et al. Dosimetric and bremsstrahlung performance of a single convergent beam for teletherapy device. Phys. Med. (2016), http://dx.doi.org/10.1016/j.ejmp.2016.10.003

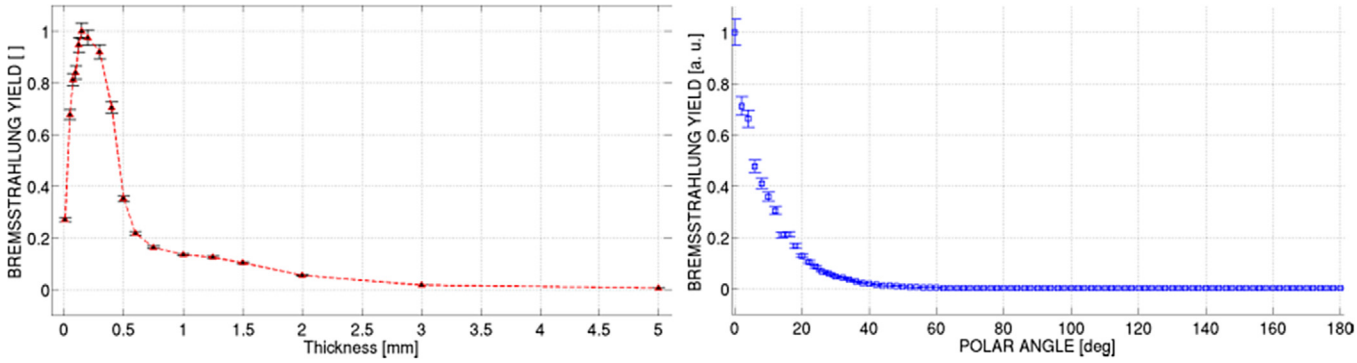

Fig. 2. Bremsstrahlung yield for different W anode thicknesses, normalized to the maximum that is 6.11×10^{10} photons per mA per second for 0.15 mm thickness, (left) and angular distribution for W anode 1 mm thick (right) due to collision of 6 MeV electrons.

Table 1
Percentage of transmitted photon flux calculated at focal spot for 6 MeV electrons and 3 mm W anode. Normalization at 100% was introduced for the limit case corresponding to absence of collimation system.

Septa aperture [°]	Flux [%]
0.5	1.9
1.0	5.6
1.5	9.4
2.0	13.1

presents typical results for the effects of collimator septa and filters calculated in air at focal spot.

After exhaustive characterization of the performance for different devices of the prototype, as reported in Figs. 2–4, it was finally possible to establish the optimal design once physical properties of its output were known. This was necessary to be able to proceed with the characterization of dosimetry.

Both analytical and stochastic approaches were used to evaluate dosimetric performances in terms of expressions (2) and (3). As described above, the output of any configuration for the device dedicated to produce the convergent beam investigated with MC simulation was the complete phase state $\Psi(\boldsymbol{r}, E, \boldsymbol{\Omega}, t)$. Then, further simulations devoted to dosimetry purposes could be started from this information, avoiding the inversion of computation time necessary to produce the convergent beam. Dosimetry calculations were performed using the physical properties of one possible configuration (1 mm W anode, 2 mm Cu filtration and 1° circular collimation) for the convergent photon beam obtained with the prototype for the irradiation of a 200 mm side cubic water equivalent phantom. For convenience, the phantom was centred at the focal spot of the prototype, which was set to 100 cm. Dose distribution was calculated using the corresponding spectrum within the phantom at voxel level (1 mm × 1 mm × 1 mm for analytical and 2 mm × 2 mm × 2 mm for MC) in order to attain 3D mapping. Fig. 5 reports in-depth dose profiles obtained by the analytical and MC approaches. The image below corresponding to a log scale graph helps to better appreciate quantitative differences.

These results, presented in Fig. 5, were also obtained for different electron beam energies in the range of 0.6–6 MeV. Then, calculations of 3D dose distributions were carried out for a setup consisting of 6 small spherical (2 mm diameter) targets close to the isocenter distributed on the edge of a diamond (regular tetrahedron). The setup consists of a superposition of 6 different irradiations equally weighted, placing successively the focus at the centre of each target.

Fig. 6 reports the results obtained with the FLUKA code for the prototype generating convergent photon beams using 2 MeV electron beam, 30° semi-aperture of a 1 mm tungsten anode, inserting 10 mm iron filter and collimating with 1 mm^2 pin-hole grid. Similar results are obtained for different electron energies. As mentioned, the capability of the device to produce convergent beams and therefore regions of high dose concentration is quite independent of electron energy. However, dose rate may vary strongly according to electron energy as well as other device's components and parameters, like collimation and filtration.

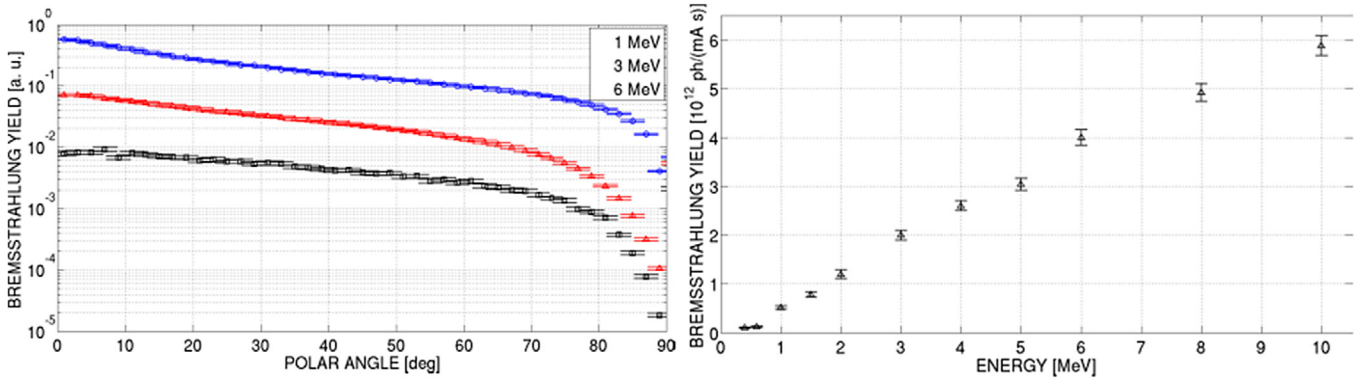

Fig. 3. Angular distribution for different electron energies (left) and total flux, expressed in photons per milli-Ampere and second of incident electron beam (right) of bremsstrahlung produced by 1 mm W anode, no filtration system.

Please cite this article in press as: Figueroa RG et al. Dosimetric and bremsstrahlung performance of a single convergent beam for teletherapy device. Phys. Med. (2016), http://dx.doi.org/10.1016/j.ejmp.2016.10.003

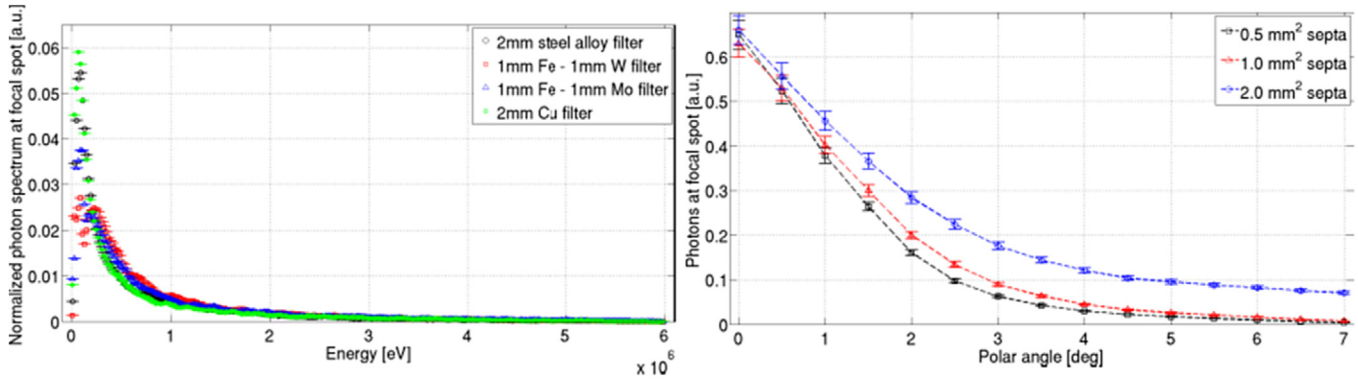

Fig. 4. Effect of filter and collimator on energy (left) and angular (right) distributions of bremsstrahlung yield at the isocenter for 1 mm W anode irradiated by 6 MeV electron beam.

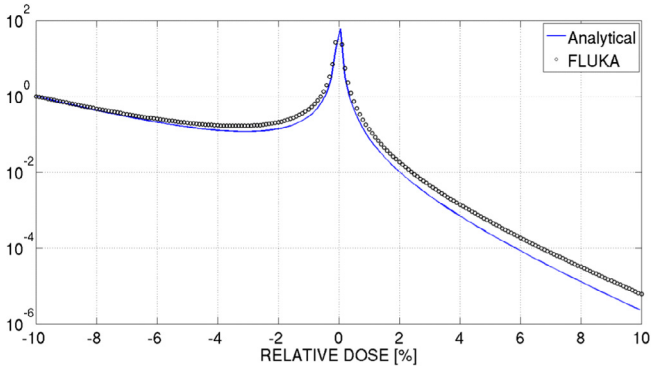

Fig. 5. In-depth dose profile along central axis obtained with analytical (solid line) and FLUKA (circles) corresponding to a 6 MeV electron current in the prototype. Profiles are normalized to entrance dose. Statistical uncertainties in FLUKA simulations for dosimetry purposes are less than 0.1%.

4. Discussion

It was observed that anode material and thickness strongly affect the bremsstrahlung yield, as expected. Particularly, Fig. 2 reports the case of 6 MeV electron current colliding with a shell anode having different thicknesses, showing that approximately 0.15 mm may correspond to the maximum bremsstrahlung yield. At this point it must be mentioned that the relevant issue for this work is photon flux at focal spot.

It was found that angular distribution of the bremsstrahlung yield concentrates the emission mainly in the forward direction, as reported in Figs. 2 and 3. In fact, the maximum of the distribution corresponds to the direction defined by the incident photon (0°), as expected. This property represents one of the main strategies for the design of a single convergent X-ray beam.

According to the results summarized in Table 1, the size of the septa affects the photon flux that is finally emitted by the prototype. Larger apertures correspond with larger percentages of transmission; whereas almost point pin-hole collimation reduces the total photon flux and consequently the dose rate for the dosimetric performance. On the other hand, less collimated "*beamlets*" produce sparser dose distributions around the focal spot, because minor differences in incident directions avoid maximum energy fluence concentration.

Figs. 2 and 3 show how the kinetic energy of incident electrons influences the angular distribution of bremsstrahlung emission. As established in Eq. (1) bremsstrahlung yield increases for higher electron energies. Furthermore, the angular distribution becomes more concentrated on the incident direction for high electron ener-

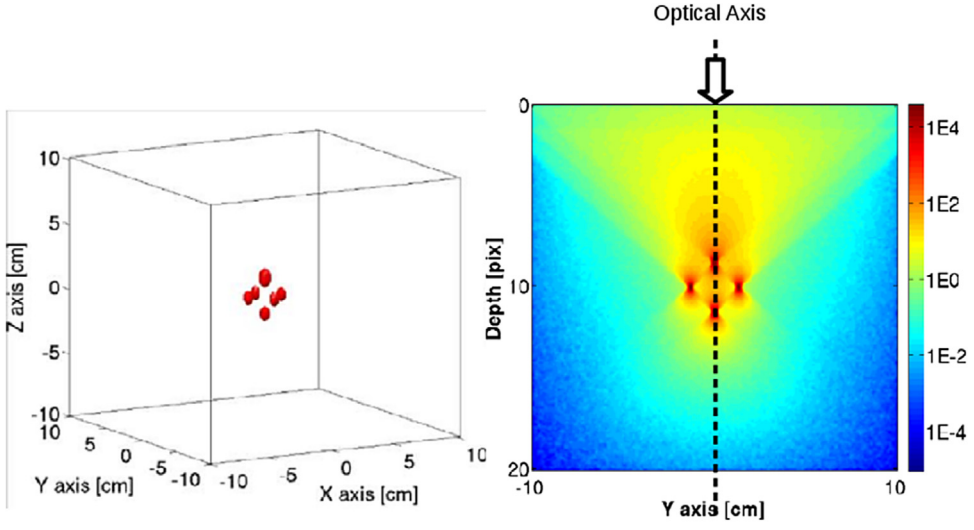

Fig. 6. Surface enclosing 90% isodose (left) and dose distribution, colours in logarithmic scale for visualization purposes (red or high and blue for low dose values, respectively), in central plane x = 0 (right) obtained from the prototype operating with electron currents with energy of 2 MeV. (For interpretation of the references to color in this figure legend, the reader is referred to the web version of this article.)

Please cite this article in press as: Figueroa RG et al. Dosimetric and bremsstrahlung performance of a single convergent beam for teletherapy device. Phys. Med. (2016), http://dx.doi.org/10.1016/j.ejmp.2016.10.003

gies, as reported in Fig. 3. Although increasing the energy of the electron beam would attain larger bremsstrahlung yield, 6 MeV was considered to be a suitable choice. It is necessary to keep in mind that one of the main purposes of this work refers to investigations about the implementation of the device for producing convergent X-ray beam as an accessory to current typical linear accelerators and all of them are able to achieve 6 MeV electron beams. Additionally, the total bremsstrahlung yield is approximately 30% greater for the case of 10 MeV than the case of 6 MeV electron energy, as indicated in Fig. 3. Therefore, the proposal for a preliminary prototype is to operate a linear accelerator with voltages around 4 or 6 MV so that some complex technological features and shielding requirements may be reduced.

As mentioned, the dosimetry performance depends strongly on dose rate and convergence of incident photons, among other parameters. Hence, physical properties like energy and angular distribution of photons arriving at focal spot were considered as key parameters for further dosimetry purposes when a phantom would be exposed to the convergent beam. Fig. 4 presents the results obtained. It must be highlighted that the suitable design of the prototype avoids excessive photon flux at focal spot when reducing septa aperture. Furthermore, the effect of different filters was investigated in order to characterize the influence in dosimetry performance. It was found that filters improve the prototype because their capacity for absorbing electrons that might be able to escape from the anode and the beam hardening effect can significantly reduce the dose at irradiation surface.

The analysis of the dosimetry performance and associated outputs of the prototype clearly indicates that the prototype is indeed capable of achieving high dose concentration in small (submilimetric) volumes. A noticeable agreement was found between the analytical approach and MC simulations with the FLUKA code. Particularly, on-axis depth dose curves are nearly indistinguishable, except for some minor differences in the exit doses, as shown in Fig. 5. Moreover, it is remarkable that both analytical and stochastic methods predict dose values in focal spot being 100 times greater, approximately, with respect to the entrance dose. Although scattering effects are not taken into account in the simplified analytical approach, it must be pointed out that it represents a reliable tool for dosimetry estimations.

In summary, the overall dosimetry performance of the prototype was characterized for a wide variety of combinations that include shape, material and thickness for the anode; material and thickness for the filter, geometry and dimensions for collimation system, among others. Fig. 6 reports a typical result for the performance of the prototype irradiating a group of small targets, clearly demonstrating the capability of the single convergent beam for this purpose. These characteristics suggest that the proposed device may be a promising technique for radiotherapy treatments requiring high dose concentrations.

5. Conclusions

A prototype capable of producing convergent beams of photons for teletherapy applications was proposed, developed and characterized. Semi-analytical and stochastic approaches were developed to evaluate the operation and dosimetric performance of the prototype.

The feasibility of controlling electron trajectories to split the beam before impact with the spherical anode shell provides a suitable mechanism to create bremsstrahlung photons mainly emitted in the forward direction toward the focus. The high atomic number of the spherical anode shell allows to obtain convergent beams by means of conical apertures of the shell, between 20 and 60°. The total bremsstrahlung yield is enough for a efficient teletherapy, even for a very reduce angular aperture of pin-hole collimation grid.

It was preliminarily shown that the proposed method is capable of assessing high concentrated 3D dose distributions, which was shown to be suitable for multiple small targets irradiation.

Acknowledgments

Authors are grateful to CORFO Innova through the 12IDL1-13124 project and the MSc. Program in Medical Physics from the Universidad de La Frontera. This project was mainly supported by FONDEF ID-15i10337 project, while DI16-6008 project from Dirección de Investigación UFRO has partially contributed to this work.

References

[1] Webb S. The physical basis of IMRT and inverse planning. Brit J Radiol 2003;76:678–89.
[2] Phillips MH, Singer KM, Hounsell R. A macropencil beam model: clinical implementation for conformal and intensity modulated radiation therapy. Phys Med Biol 1999;44:1067–88.
[3] Spirou SV, Chui CS. Generation of arbitrary intensity profiles by dynamic jaws or multileaf collimators. Med Phys 1994;21:1031–41.
[4] Bassalow R, Rodebaugh R. Evaluation of six dosimetric indices for cyber knife stereotactic radiosurgery treatment planning. Med Phys 2006;33:2100.
[5] Maxim P, Fahimian B, Xing L. Image guidance on the TrueBeam STx: evaluation of CBCT imaging dose and quality. Int J Radiat Oncol Biol Phys 2011;81(2):S849–50.
[6] Mackie TR et al. Tomotherapy: a new concept for the delivery of dynamic conformal radiotherapy. Med Phys 1993;20:1709–19.
[7] Lindell B, Sievert R, Wahlberg T. A method of concentrating Roentgen rays for deep therapy (preliminary reports). Acta Radiol 1950;33:353–6.
[8] Sievert R. A Roentgen apparatus for intense Roentgen radiation of short duration intended for biophysical research work and for special treatment purposes. Acta Radiol 1950;33:328–43.
[9] Figueroa R, Valente M. Physical characterization of single convergent beam device for teletherapy: theoretical and Monte Carlo approach. Phys Med Biol 2015;60:7191–206.
[10] Figueroa R, Valente M. Convergent photon and electron beam generator. Chile Patent office 00898-11, Argentina Patent office 20120101380, International Patent System (WIPO) PCT/IB2012/051983, US patent 14/112.429.
[11] Jackson J. Classical electrodynamics. 2nd ed. J Wiley & sons, Inc; 1975.
[12] Attix F. Introduction to radiological physics and radiation dosimetry. J Wiley & sons, Inc; 1986.
[13] Valente M, Malano F, Perez P, Castro N, Carrasco F. Characterization of a megavoltage linear accelerator Bremsstrahlung by means of Monte Carlo simulations. X-ray Spectrom 2010;39(1):384–90.
[14] Sommerfeld A. Zur Quantentheorie der Spektrallinien (Fortsetzung). Ann Phys 1916;51(1):17.
[15] Battistoni G, Muraro S, Sala P, Cerutti F, Ferrari A, Roesler S, Fasso A, Ranft G. The FLUKA code: description and benchmarking. In: Proceedings of the hadronic shower simulation workshop, Fermilab 6–8 September 2006, vol. 896. p. 31–49. AIP conference proceeding.
[16] Ferrari A, Sala P, Fasso A, Ranft J. FLUKA: a multi-particle transport code. CERN-2005-10 INFN/TC_05/11, SLAC-R-773; 2005.
[17] Söderströms S, Gustafsson A, Brahme A. Few-field radiation therapy optimization in the phase space of complication-free tumor control. Int J Imaging Syst Technol 1995;6(1):91–103.